Characterization of protein lactylation in relation to cardiac metabolic reprogramming in neonatal mouse hearts

Tongyu Zhang
Nanjing University

Yingxi Zhu
Nanjing Medical University

Xiaochen Wang
Nanjing University

Danyang Chong
Nanjing Medical University

Haiquan Wang
Nanjing University

Dandan Bu
Nanjing University

Mengfei Zhao
Nanjing University

Lei Fang
Nanjing University

Chaojun Li

lichaojun@njmu.edu.cn

Nanjing University

Additional Declarations: No competing interests reported.

Abstract

Background

In mammals, the neonatal heart regenerates within a short time after birth, but adults lack this ability. The metabolic patterns of embryonic and adult hearts are completely different. We have shown that metabolic reprogramming is critical for cardiomyocyte proliferation in the neonatal heart. However, the molecular mechanism of metabolic reprogramming in neonatal heart still needs to be explored. Herein, we revealed that cardiac metabolic reprogramming could be regulated by altering global protein lactylation.

Results

4D label-free proteomics and Kla omics were performed in postnatal Day 1 (P1), 5 (P5), and 7 (P7) mouse hearts, 2297 Kla sites from 980 proteins were identified, and 1262 Kla sites from 409 proteins were quantified. Functional clustering analysis of proteins with altered Kla sites revealed that the proteins were mainly involved in metabolic processes. The Kla levels in several fatty acid oxidation-related proteins showed high expression at P5, while most glycolysis and cell cycle-related proteins were sustainedly decreased from P1-P7. Furthermore, we verified the Kla levels of several differentially modified proteins, including ACAT1, ACADL, ACADVL, PFKM, PKM and NPM1, by coimmunoprecipitation and Western blotting.

Conclusions

We reported the first comprehensive Kla map in the neonatal mouse heart, which will aid in understanding the regulatory network of metabolic reprogramming and cardiac regeneration.

Background

Heart disease is among the leading causes of death worldwide[1, 2]; however, a daunting challenge remains in developing efficient treatments for heart disease. As the most metabolically active and most mitochondrial-abundant organs, mammalian hearts pump blood and transport oxygen and nutrients to various organs throughout the body[3, 4]. Obviously, heart function is highly dependent on mitochondrial energy production, which provides the enormous ATP necessary for its continuous contractile activity[5, 6]; and most heart diseases are characterized by mitochondria-related metabolic disorders[7, 8].

The metabolic patterns of embryonic and adult hearts are completely different. The adult heart mainly uses fatty acids, which provide more than 70% of the energy in cardiomyocytes, whereas carbohydrates (glucose and lactate) are the main energy sources of the embryonic heart[9–12]. In the neonatal heart, there is increased energy demand to meet the high-load beating function, and cardiac metabolism

gradually switches from glycolysis to fatty acid oxidation (FAO) within a short period after birth[10, 13–15]. On the other hand, the adult heart can barely regenerate, while embryonic and neonatal hearts can regenerate efficiently following apical resection as well as myocardial infarction (MI); this ability for cardiomyocytes to proliferate is lost within 7 days after birth[16–19]. Subsequently, metabolic reprogramming occurred simultaneously with the loss in regenerative potential of the neonatal heart within the 7-d time window. In our previous work, we have shown that metabolic reprogramming is critical for cardiomyocyte proliferation in the neonatal heart[20]; however, the underlying mechanism of metabolic remodeling remains unknown.

Lysine lactylation (Kla), as a novel PTM, has been reported to be lactate-derived and regulates gene transcription and protein function by modifying histones and functional proteins[21, 22]. Lactate in the embryonic heart is abundant due to active glycolysis. However, along with metabolic reprogramming in the neonatal heart, the lactate level largely decreases. To uncover the global alteration of proteins lactylation and the underlying relationship between proteins lactylation and metabolic reprogramming in the neonatal heart, we adopted a relatively new acquisition strategy, 4D label-free proteomics and Kla omics, and compared the protein and Kla levels in P1, P5 and P7 mouse hearts. This comprehensive characterization of Kla might provide a new direction for research on cardiac regeneration and heart diseases.

Results

Bioinformatics analysis of proteins with dysregulated expression levels showed metabolic reprogramming in neonatal hearts

To determine the underlying correlations between neonatal cardiac regeneration and metabolic reprogramming in the perinatal stage, we profiled protein expression changes during the first 7 days at P1, P5, and P7 by general proteomics (Fig. 1A). In total, 5303 proteins were identified, among which 5104 proteins were quantified (Fig. 1B). When setting the fold change > 1.5, p < 0.05 as a differentially regulated protein, 388 proteins were upregulated and 319 proteins were downregulated in P5/P1, 484 proteins were upregulated and 426 proteins were downregulated in P7/P1, and 64 proteins were upregulated and 86 proteins were downregulated in P7/P5 (Fig. 1C), indicating dramatic changes in protein expression occurred in the neonatal heart.

To further understand the characteristics and functions of the altered proteins, we performed bioinformatics analyses to reveal the changes in protein expression in neonatal hearts. Gene set variation analysis (GSVA) for the 4721 proteins quantified at all 3 time points to recognized the alteration of different cellular processes, we selected C2 gene set in MSigDB as the reference data set and adopted "Poisson" method. With the development of neonatal heart, GSVA showed that glycolysis and gluconeogenesis, the p53 signaling pathway, the cell cycle and DNA replication were downregulated,

while the PPAR signaling pathway, fatty acid metabolism, biosynthesis of unsaturated fatty acids and cardiac muscle contraction were upregulated (Figure S1A). These results indicated that fatty acid metabolism and cardiac muscle contraction were increased in neonatal hearts, whereas glycolysis and the cell cycle were inhibited, which might lead to the loss in cardiac regenerative capacity.

To explored the dynamic changes of protein level in neonatal heart, series test of cluster (STC) analysis was performed to recognize distinct protein clusters with similar expression trends, which might perform similar biological functions. In total, the 4721 proteins were divided into 8 clusters with similar coexpression trends (Cluster 1–8), accounting for 389, 309, 393, 326, 605, 1096, 807 and 796 proteins, respectively (Fig. 1D). Cluster 1 and 2 exhibited a decrease at P5, followed by an increase at P7, whereas clusters 3 and 4 displayed an increase at P5, subsequently followed by a decrease at P7. Cluster 5 was characterized by upregulated proteins, cluster 6 showed a decline at P5 but remained stable at P7. Cluster 7 displayed an upregulation at P5, which persisted at P7, and cluster 8 was primarily composed of downregulated proteins. Hence, we combined cluster 1 and cluster 2 to form C1, merged cluster 3 and cluster 4 to create C2, and assigned C3 to cluster 5, C4 to cluster 6, C5 to cluster 7, and C6 to cluster 8 for bioinformatics analyses. Through KEGG pathway analysis of the 6 clusters, we found that glycolysis was mainly identified in C4, while the Citrate cycle (TCA cycle), Oxidative phosphorylation, Fatty aicd metabolism, Fatty aicd degradation and PPAR signaling pathway were significantly enriched in C5. Additionally, Cell cycle, DNA replication, Mismatch repair and Spliceosome were prominently featured in C4 and C6 (Fig. 1E).

Furthermore, GO enrichment analyses were conductedfor these 6 clusters, with the P.adj < 0.05. In the biological process category, the outcomes revealed that glycolytic process was primarily associated with C4, tricarboxylic acid cycle, oxidative phosphorylation, lipid metabolic process, fatty acid metabolic process and cellular respiration were mainly identified in C5, signifying that glycolysis was suppressed and fatty acid oxidation was augmented in neonatal hearts. Moreover, DNA replication, DNA repair, chromatin remodeling, cell cycle, RNA splicing and ribosome biogenesis were enriched in C4 and C6, indicating that the cell cycle and cardiomyocyte proliferation were hindered in neonatal hearts (Figure S1B). In the cellular component category, chromosome (telomeric region), spliceosomal complex, nuclear matrix, cytosolic ribosome and ribonucleoprotein complex were discerned in C4 and C6, whereas C5 mainly include mitochondrial inner membrane, mitochondrial respiratory chain complex (I, III and IV), peroxisome and respiratory chain (Figure S1C). Additionally, in the molecular function category, C5 was primarily characterized by fatty-acyl-CoA binding, lipid binding and NAD binding, while RNA binding, actin binding and ribosome binding fell into C4 and C6 (Figure S1D). This analysis identified several proteins with the Log_2 FC > Log_2 1.2, glycolytic proteins mainly fell into C4 and C6, such as ADH5, GALM, PKM, TPI1, ALDOC, PGAM1 and PGK1, which showed decreased glycolysis in the neonatal heart (Fig. 1F). FAO-related proteins were enriched in C3 and C5, such as CPT2, CPT1β, ACSL1, ACADL and ACAT1, which were increased (Fig. 1G). In addition, the expression of proteins involved in the cell cycle, cyclin family and MCM family was reduced in the neonatal heart (Fig. 1H). Above all, these results demonstrated that

metabolic remodeling occurred in the 7-d time window of the neonatal heart, accompanied by cell cycle arrest.

Global protein Kla levels were decreased with metabolic reprogramming during the perinatal stage

To establish the comprehensive profiling of the protein Kla in the neonatal heart, we selected 4 time points to detect the protein Kla abundance in perinatal hearts and embryonic Day 18.5 (E18.5), P1, P5, and P7 hearts (Fig. 2A-2B and Figure S2). We found that the Kla abundance of the P1 heart was similar to that of E18.5, which was consistent with the observation that a proper regenerative capacity is retained by P1 heart [16]. In addition, there was a sharp decline in Kla abundance in P5 and P7 hearts. This accompanying protein Kla alteration, metabolic reprogramming and cardiac regenerative ability loss in the postnatal heart indicates an underlying correlation between protein Kla and cardiac regeneration.

Thus, we selected P1, P5 and P7 hearts of C57BL6/J mice to perform Kla omics analysis. The Kla levels of Kla sites were detected by normalizing the Kla peptide abundance with the protein abundance based on the proteomics and Kla omics analyses. To validate the quality of the MS data, principal component analysis (PCA) showed that the 3 samples, P1, P5 and P7, were separated into three distinct quadrants, indicating significant differences in the protein Kla status of P1, P5 and P7 hearts (Figure S3A), and the peptide mass error of most peptides was less than 5 ppm, which means that the mass accuracy of the MS data was acceptable (Figure S3B). Finally, for most of the identified proteins, the number of Kla sites per protein was 1 to 3 (Figure S3C).

The Kla sites were identified and quantified through database searching, and further bioinformatics analysis was performed to reveal the marked alterations in normalized Kla levels in the metabolic remodeling period in mice. In total, 2297 lactylation sites from 980 proteins were identified, among which 1262 lactylation sites from 409 proteins were quantified (Fig. 2C). The postnatal standardization of protein lactylation levels exhibited a downward trend in murine cardiac tissue (Fig. 2D). And we generated a heatmap of lactylation omics, wherein a minority of protein sites displayed augmented lactylation level, yet the most proteins Kla level in heart decreased postnatally (Fig. 2E). Taken together, these results suggested that there was a global decrease in the protein Kla level accompanied by metabolic reprogramming during the perinatal stage.

Functional enrichment analysis of proteins with dysregulated Kla sites

To further understand the characteristics and function of the proteins with Kla sites, we first identified the Kla sites that were expressed at all 3 time points and obtained 782 differentially modified Kla sites in the postnatal heart. We applied several functional enrichment analyses to examine the dynamics of Kla changes in the neonatal heart. STC analysis for the differentially modified proteins grouped the 782 Kla sites into 10 coexpression trend clusters. Cluster 1, 2 and 3 were dominated by downregulated proteins,

while cluster 4 and 5 mainly contained upregulated proteins, cluster 6 and 7 exhibited an increase at P5 followed by attenuation at P7, with the Kla level remaining greater than that of P1, cluster 8 and 9 demonstrated a parallel expression pattern to cluster 6 and 7, however, the Kla level at P7 was lower than that of P1. Cluster 10 was comprised of a mere three proteins Kla sites, and the sample size was deemed insufficient for bioinformatics analysis, consequently, cluster 10 was disregarded. Therefore, we amalgamated cluster 1, 2 and 3 to generate C1, combined cluster 4 and 5 to form C2, and designated cluster 6 and 7 as C3, cluster 8 and 9 as C4 for subsequent bioinformatics analyses. C1 and C4 contained 686 of all 782 Kla sites, suggesting that Kla level of most proteins were decreased after birth, which was consistent with Fig. 2 (Fig. 3A). Through KEGG enrichment analysis of these 4 clusters, glycolysis, protein translation (ribosome) and spliceosome were enriched in C1 and C4, which displayed a general decline in neonatal hearts. C2 showed a significant enrichment of cardiac muscle contraction and citrate cycle (TCA cycle). Furthermore, fatty acid degradation and PPAR signaling pathway were identified in C3 (Fig. 3B).

GO-based functional enrichment analysis was performed to elucidate proteins in these 4 clusters. When setting the P.adj < 0.05, the biological process category revealed significant enrichments of cytoplasmic translation, protein folding, actin cytoskeleton organization, glycolytic process, and canonical glycolysis in C1 and C4. In contrast, lipid metabolic process was primarily associated with C3 (Fig. 3C). Correspondingly, the cellular component category unveiled processes related to protein biosynthesis and cell proliferation, such as ribosome, cytoskeleton, cytosolic ribosome, and ribonucleoprotein complex, in C1 and C4 (Fig. 3D). Furthermore, in the molecular function category, double-stranded DNA binding, RNA binding, structural constituent of ribosome, and protein binding were identified in C1 and C4, while fatty-acyl-CoA binding and electron carrier activity were predominantly involved in C3 (Fig. 3E). Taken together, proteins Kla mainly participated in metabolic pathways, proteins biosynthesis and cell proliferation.

In addition, we performed GO-based enrichment analysis of C1-C4 with P.adj < 0.05 to determine the other pathways containing lactylated proteins and discovered that protein Kla was implicated in other cellular processes apart from metabolism and cell cycle (Figure S4). We observed the participation of Kla in cellular processes pertaining to mitochondrial metabolism, cytoskeleton, and protein biosynthesis. Thus, these results suggested that nonhistone Kla might mainly modulate mitochondrial metabolism and protein biosynthesis.

With the underlying association of metabolic reprogramming and proteins Kla, we analyzed the alteration in metabolism-related protein Kla levels. C1 and C4 contained the Kla sites of glycolytic proteins PGAM2, PFKP, PKM, PGK1 and ALDOA. In addition to glycolytic proteins, proteins involved in DNA replication, such as Structural Maintenance of Chromosomes 3 (SMC3), Replication Protein A1 (RPA1) and Nucleophosmin 1 (NPM1), and ribosomal proteins family, RPL3, RPL6, RPS6 and RPS7, were also identified in C1 and C4. While C3 included critical regulators of fatty acid oxidation, FABP3, ECI1 and ACADVL.

Glycolysis and cell proliferation showed a positive correlation between proteomics and Kla omics, while FAO showed a negative correlation

To obtain a more comprehensive understanding of the implications of protein Kla in the neonatal 7-day time frame, we conducted a Pearson correlation coefficient analysis between proteomics and Kla omics to profile the correlation between the protein Kla level and the underlying cellular processes.

The Pearson correlation analysis demonstrated a clearly positive and negative correlation between protein abundance and Kla level of the modified sites (Fig. 4A). When we setting the absolute value of Pearson correlation coefficient 0.8, we observed that the number of Kla sites exhibiting a positive correlation (172) was less than that with a negative correlation (208), but the number of proteins showing a positive correlation (109) outweighed those with negative correlation (81), indicated that the positively correlated modification sites were extensively distributed (Fig. 4B). Meanwhile, the Venn diagram displayed 109 positive correlated proteins and 81 negative correlated proteins, 10 of them were in the intersection, which contained both positive and negative correlated Kla sites (Fig. 4C).

The KEGG pathway analysis revealed that glycolysis/gluconeogenesis, ribosome, DNA replication and cell cycle were enriched in positive correlation group, while PPAR signaling pathway, TCA cycle, fatty acid degradation and oxidative phosphorylation were identified in negative correlation group (Fig. 4D). Besides, we conducted functional enrichment analysis of the positive correlation group based on GO, and found that the protein abundance of mRNA processing, ribosome biogenesis, DNA biosynthetic process and glycolytic process were positively correlated with their Kla level (Fig. 4E). And the GO analysis of the negative correlation group showed that the group comprised ATP metabolic process, cellular respiration, TCA cycle, fatty acid beta-oxidation and oxidative phosphorylation (Fig. 4F).

To further explore the potential role of Kla in cardiac metabolism and cell proliferation, we extracted proteins with differentially regulated Kla sites (Log_2 FC > Log_2 1.2) from glycolysis, FAO and the cell cycle. According to the expression pattern, we could classify glycolytic proteins into the following groups (Fig. 5A and 5C): class 1 included PFKP, ENO1, PKM and ALDOA, the protein level of class 1 proteins declined after birth, and the Kla level of class 1 also decreased. Class 2 identified DLD, ENO3 and PDHA1, which showed increased protein expression, while the Kla level of class 2 was variable; for example, ENO3 K275 decreased, but ENO3 K80 increased at P5 and then decreased at P7. Similarly, for FAO, there were 3 classes of proteins (Fig. 5B and 5D). In class 3, the protein abundance of ACADVL, ACADL, ACADM, ECI1 and ACSL1 was increased, while their Kla level was increased at P5 and then attenuated at P7, consistent with the enhanced FAO in the postnatal heart. According to our proteomic results, FAO-related protein expression was increased after birth; thus, we suspected that at P5, the upregulated Kla level might contribute to the increased protein expression and function. Class 4 contained HADH, HADHB, ACAA2 and ACADS, and the protein level was enhanced, but the Kla level was reduced in the 7-d time window after birth. In class 5 FAO proteins, the different Kla sites showed different expression trends in HADHA and ACAT1. The Kla levels at K569, K634, K519, K644, K415, K60 and K406 of HADHA were decreased in P5 and P7 hearts, whereas the K334, K284 and K390 of HADHA were similar to the class 3 proteins. There was a transition of the Kla level at P5. In addition to the Kla sites of ACAT1, K248 and K265 showing diverse statuses after birth, K248 showed an increase at P5 and then an attenuation at P7,

while the Kla level of K265 was decreased after birth. Taken together, these results implied that the effect of Kla might be flexible and could have different functions at different Kla sites.

However, in regard to cell cycle-related proteins, we identified decreased protein expression in proteomics (Fig. 1H), but our Kla omics results showed that there were very few lactylated proteins involved in the cell cycle. Only a small minority of the modified proteins related to the cell cycle were identified, such as SMC3, RPA1, NPM1 and nuclear DNA helicase II (DHX9) (Fig. 5E), suggesting that protein lactylation might prefer to participate in cardiac metabolic activity compared with the cell cycle.

Moreover, we observed that the glycolytic proteins PFKP and ENO1 showed a positive correlation between the protein level and Kla level (Fig. 5F and 5G), and the DNA replication-related proteins SMC3 and NPM1 presented a positive correlation (Fig. 5H and 5I), while the FAO enzyme ACAT1 showed a negative correlation (Fig. 5J). The Kla level of ACADL K338 was positively correlated with the ACADL expression level, but ACADL K322 showed a negative correlation (Fig. 5K). Above all, these results suggested that in the neonatal heart, protein lactylation mainly participate in metabolic pathways, the correlation between protein and Kla level was positive in glycolysis and the cell cycle, and the correlation was negative in the PPAR signaling pathway and fatty acid β-oxidation.

Verification of proteins with dysregulated Kla sites

To verify the dynamic alteration of protein Kla levels in the 7-d time window after birth, several proteins with dysregulated Kla sites were selected, and the Kla omics results were validated. In the neonatal heart, there was increased fatty acid β-oxidation and decreased glycolysis, but the alteration of the Kla levels of these proteins varied (Fig. 6A). To validate the identification of lysine lactylation, we extracted the mass spectra of several Kla modified peptides of selected proteins (Figure S5-S8). However, due to the limitations in detecting Kla levels at specific sites, we detected the overall Kla abundance of selected proteins through coimmunoprecipitation and Western blot, and then normalized the Kla abundance with the corresponding protein expression level. Acyl-CoA dehydrogenase long chain (ACADL), Acyl-CoA dehydrogenase very long chain (ACADVL) and Acetyl-CoA acetyltransferase (ACAT1) are important enzymes that catalyze the mitochondrial β-oxidation pathway. The proteomics showed that the protein expression levels of ACADL, ACADVL and ACAT1 were increased at P5 and P7 (Fig. 5B). And we found that both the Kla abundance (Top band of Fig. 6B-C and Figure S9 A-B) and the normalized Kla level (Figure S10 A-B) of ACADL and ACAT1 were decreased in neonatal hearts. Besides, the Kla abundance of ACADVL increased at P5 and then declined at P7 (Top band of Fig. 6D and Figure S9C), aligning with the Kla omics data, however, when we normalized the Kla abundance by protein abundance, the Kla level of ACADVL showed a decrease at both P5 and P7 (Figure S10C), potentially due to a marked upregulation of the protein abundance at P5 and P7. PFKM and PKM are critical glycolytic enzymes, we found that in neonatal hearts, both the Kla abundance (Top band of Fig. 6E and Figure S9D) and the normalized Kla level of PFKM were decreased (Figure S10D), which was consistent with our omics data. Although the Kla abundance of PKM was decreased at P5 and P7 (Top band of Fig. 6F and Figure S9E), the Kla level of

PKM after normalization was increased at P5 and decreased at P7 (Figure S10E), might result from the significant downregulation of the protein abundance at P5.

NPM1 is involved in various cellular processes, such as ribosome biogenesis, histone assembly, centrosome duplication, cell proliferation, and regulation of the tumor suppressor p53/TP53. We detected the Kla level of NPM1 after birth, which was similar with PKM, the Kla abundance and the protein expression level of NPM1 were both decreased at P7 (Fig. 6G and Figure S9F), while the Kla level after normalization showed upregulated at P5 and downregualted at P7 (Figure S10F). Moreover, we also detected the Kla level of 14-3-3z, which involved in many vital cellular processes such as metabolism, signal transduction and cell cycle regulation[23–26], we found that Kla abundance of 14-3-3z was decreased after birth (Top band of Figure S11), aligning with our Kla omics data. Above all, the verification of proteins with dysregulated Kla sites proved the reliability of our MS data. These proteins are involved in diverse cellular processes and thus elucidate the global alteration in Kla in postnatal hearts.

Discussion

The limited regenerative capacity of the adult mammalian heart leads to the high lethality of CVDs[27], and the complicated mechanism of cardiac regeneration inhibits the exploration of efficient therapies for heart injury. Numerous studies in the last few decades have shown that cardiac regeneration is regulated by a complex network that involves metabolism, signaling pathways, hormones, oxygen, the peripheral environment and many other regulators[11, 28–31]. Metabolic homeostasis is crucial for heart function, and the disturbance of metabolism is an important cause for the development of cardiomyopathies and cardiovascular diseases. Thus, expanding the knowledge of cardiac metabolism and cardiac regenerative processes has important clinical interest.

Our previous studies have shown that metabolic remodeling occurred from glycolysis to FAO in perinatal hearts via transcriptome and metabolome analyses, which was accompanied by a loss in cardiac regenerative capacity, implying the underlying relationship between cardiac metabolism and regeneration[20]. Glycolysis has been reported to regulate the cell cycle and promote cardiomyocyte proliferation to accomplish cardiac regeneration[32].

As a novel PTM, Kla is closely related to metabolism, especially glycolysis and FAO. However, the role of Kla in metabolic remodeling in the perinatal heart is unknown, and most of the studies mainly revealed the regulation of histone Kla on gene expression, while studies on nonhistone Kla are rare.

In this study, we verified metabolic remodeling through proteomic analysis and reported that the global protein Kla level was decreased in neonatal hearts (Fig. 2A and 2B). Thus, to describe the protein Kla more accurately, we established the global map of proteins Kla in neonatal hearts of mice by multiomics analysis, combining the general proteomic and Kla omics analysis. We found that the alteration of Kla mainly occurred in mitochondria and participated in a series of metabolic processes, including fatty acid β-oxidation, glycolysis, the TCA cycle and oxidative phosphorylation. In addition, we enriched the proteins

with dysregulated Kla sites in protein translation, such as ribosomal proteins. Nevertheless, we found that only a few cell cycle-related proteins were identified, such as SMC3, RPA1 and NPM1, suggesting that protein lactylation was more likely to regulate cardiac metabolism.

In recent years, the study of the biological function of Kla has increased because of the Warburg effect in tumor cells. Subsequent studies confirmed that protein lactylation modification is an important mechanism of lactate function, which is involved in glycolytic-related cell functions[33], macrophage polarization[34], nervous system regulation[35] and other important biological processes. It was reported that Glis1, a transcription factor, could amplify epigenomic signals through a unique metabolic remodeling mechanism. The amplification was not accomplished at the genomic level but rather at the "metabolic" level to form an "epigenome-metabolome-epigenome" cascade, which affected the determination of cell fate. The histone Kla, which links the metabolome to the epigenome, plays a central role in this regulatory process[33]. In addition, the metabolic regulation of Kla in Trypanosoma brucei was reported. Trypanosoma brucei lacks the TCA cycle, glycolysis is the main energy metabolic pathway, 25 Kla sites were identified on seven glycolytic enzymes, and lactylation modification was mainly found in the catalytic site of the enzyme, which may be related to the regulation of enzyme activity[36]. Therefore, according to our Kla omics and proteomics data, nonhistones Kla, which are derived from glycolysis, are mainly involved in the regulation of glycolysis and other mitochondrial metabolic processes.

Furthermore, we found that in the neonatal heart, the correlation between proteomics and Kla omics was positive for glycolysis and the cell cycle and negative for the FAO and PPAR signaling pathways. Interestingly, the protein abundance of ACADVL, ACADL, ACADM, ECI1 and ACSL1 was increased to promote FAO in neonatal hearts, while the Kla level of their Kla sites was increased at P5. For example, K333 and K338 of ACADL were upregulated at P5 compared with P1, which implied that at P5, the upregulated Kla levels of ACADVL, ACADL and ACSL1 might positively regulate their protein stability and enzyme activity. In addition, the different Kla sites showed different trends for Kla in FAO- and glycolysis-related proteins, such as HADHA and ACAT1. The Kla levels at K569, K634, K519, K644, K415, K60 and K406 of HADHA decreased after birth, whereas at K334, K284 and K390 of HADHA, there was a transition of the Kla level at P5. K248 and K265 of ACAT1 also showed diverse statuses; K248 showed an increase at P5, while the Kla level of K265 was decreased. The glycolytic proteins DLD, ENO3 and PDHA1 showed increased protein expression in the neonatal heart, and their Kla level was variable; for example, ENO3 K275 was decreased, while ENO3 K80 was increased at P5. Therefore, these results indicated that the effect of Kla might not be invariable; it could exhibit different functions at different Kla sites.

It was reported that the lactylated glycolytic enzyme ALDOA is conserved in a variety of human tumor cell lines. Researchers found that the enzyme activity was significantly reduced after lactylation at ALDOA K147, revealing the feedback regulation mechanism in which the activity of glycolysis was inhibited by covalently modifying the upstream metabolic enzymes in the glycolytic pathway[37]. According to our Kla omics data, the Kla level of ALDOA K147 was decreased in the neonatal heart, while the protein expression of ALDOA was decreased at P5 but increased slightly at P7 (Fig. 4A and 4C), which means

that the decline in Kla at ALDOA K147 might contribute to the increased protein stability and enzyme activity at P7.

Taking the results together, we speculated that Kla might perform different functions at different Kla sites, thereby modulating protein stability and enzyme activity, which provides a new strategy for research on cardiac metabolic disorders and cardiac regeneration. However, the effect of protein Kla on the function of these proteins remains unclear, and further research on how Kla regulates protein function would aid in understanding the role of protein Kla in cellular processes in this study.

Conclusions

This study reports the first comprehensive Kla map in the neonatal mouse heart via 4D label-free proteomics and Kla omics, which suggests that nonhistone proteins lactylation occurs throughout the whole proteome, especially involves metabolic processes such as glycolysis and FAO. And we describe the alteration of proteins Kla level accompanies with the metabolic reprogramming from glycolysis to FAO and the loss of cardiac regenerative capacity during perinatal stage. Furthermore, the changes of Kla in different pathways vary, which means that Kla might represent various functions at different Kla sites of different proteins. Our study provides a new view for the understanding of metabolic reprogramming and cardiac regeneration in mouse heart.

Materials and methods

Animals

C57BL/6 J mice were obtained from the Model Animal Research Center of Nanjing University. In this study, 16 P1 hearts, 8 P5 hearts and 6 P7 hearts were pooled for each sample to perform proteomic and Kla omic analyses. All animals were maintained on a normal 12 h/12 h light/dark cycle on a regular chow diet. The mice were given access to water *ad libitum*. Mice were sacrificed under isoflurane anesthesia followed by cervical dislocation at the indicated time points. All animal experiments conformed to the NIH guidelines (Guide for the Care and Use of Laboratory Animals) and were carried out in accordance with the protocol approved by the Animal Care and Use Committee at the Model Animal Research Center of Nanjing University in Nanjing, China.

Protein extraction

The samples were removed from − 80°C, weighed into a precooled mortar with liquid nitrogen, and ground to powder with liquid nitrogen. Each group of samples was lysed by adding 4 times the volume of lysis buffer (1% Triton X-100, 1% protease inhibitor, 3 μM TSA, 50 mM NAM) and ultrasonic lysis. After centrifugation at 4°C and 12,000 × g for 10 min to remove cell debris, the supernatant was transferred to a new centrifuge tube for protein concentration determination using a BCA kit.

Protein digestion

Equal amounts of each sample protein were taken for enzymatic digestion, and the volume was adjusted to uniformity with lysis solution. A final concentration of 20% TCA was slowly added, vortexed, mixed, and precipitated for 2 h at 4°C. At 4500 g, the samples were centrifuged for 5 min, the supernatant was discarded, and the precipitate was washed with prechilled acetone 2–3 times. After the precipitate was dried, TEAB was added at a final concentration of 200 mM, the precipitate was sonicated and broken up, trypsin was added at a ratio of 1:50 (protease: protein, m/m), and the precipitate was digested overnight. Dithiothreitol (DTT) was added to a final concentration of 5 mM and reduced for 30 min at 56°C. Iodoacetamide (IAA) was added to a final concentration of 11 mM, incubated for 15 min at room temperature and protected from light.

Lactylated peptide enrichment

The peptides were dissolved in IP buffer solution (100 mM NaCl, 1 mM EDTA, 50 mM Tris-HCl, 0.5% NP-40, pH 8.0), and the supernatant was transferred to prewashed lactylated resin (antibody resin No. (PTM-1404). The antibody was incubated on a rotary shaker at 4°C with gentle shaking and overnight incubation. After incubation, the resin was washed four times with IP buffer solution and twice with deionized water. The peptides bound to the resin were eluted three times with 0.1% trifluoroacetic acid eluent, and the eluate was collected, vacuum frozen and dried. The eluate was collected and vacuum freeze-dried. After drying, the peptide was desalted according to C18 ZipTips instructions and vacuum freeze dried for LC−MS/MS analysis.

LC−MS/MS analysis

The peptides were dissolved with liquid chromatography mobile phase A and then separated using a NanoElute ultrahigh-performance liquid phase system. Mobile phase A was an aqueous solution containing 0.1% formic acid and 2% acetonitrile; mobile phase B was a solution containing 0.1% formic acid and 100% acetonitrile. The liquid phase gradient settings were as follows: 0−40 min, 6%-24% B; 40−52 min, 24%-32% B; 52−56 min, 32%-80% B; 56−60 min, 80% B, and the flow rate was maintained at 450 nL/min. The peptides were separated by the UHPLC system, injected into the capillary ion source for ionization and then analyzed by timsTOF Pro mass spectrometry. The ion source voltage was set at 1.7 kV, and the peptide parent ions and their secondary fragments were detected and analyzed using high-resolution TOF. Precursors and fragments were analyzed at the TOF detector, with a MS/MS scan range from 100 to 1700 m/z. The timsTOF Pro was operated in parallel accumulation serial fragmentation (PASEF) mode. Precursors with charge states 0 to 5 were selected for fragmentation, and 10 PASEF-MS/MS scans were acquired per cycle. The charge number was set as 0−5, where 0 represented the 'Unknown charge state', most proteins with a charge number of 1 were excluded, proteins with an unknown charge state or with charge numbers of 2−5 were selected for further analysis. The dynamic exclusion was set to 30 s. Column for peptide separations: 1.9 μm/120 Å ReproSilPurC18 resins (Dr. Maisch GmbH, Ammerbuch, Germany)/ReproSil-Pur Basic C18 column (1.9μm, 100μm x 25cm).

Bioinformatics analyses of general proteomics

Enrichment analysis of Gene Ontology and the Kyoto Encyclopedia of Genes and Genomes (KEGG) pathway was performed for proteins with dysregulated expression levels. Briefly, proteins with dysregulated expression levels were classified by GO annotation into three categories: biological process, cellular compartment and molecular function. Similarly, the KEGG database was used to identify enriched pathways in proteins with dysregulated expression levels against all identified proteins. For each GO, KEGG pathway a two-tailed Fisher's exact test was employed to test the enrichment of proteins with dysregulated expression levels. The GO, KEGG pathway with a corrected p value < 0.05 is considered significant.

Bioinformatics analyses of proteins with dysregulated Kla sites

To eliminate the effect of protein expression on lactylation modification, we also studied the overall protein expression levels using quantitative proteomics. Then, we standardized the Kla-modified peptide intensity of proteomics and analyzed the proteins with differential Kla levels in P1, P5, and P7 with a series analysis of clusters by Mfuzz. Then, we annotated the Kla-modified proteins in each cluster with Gene Ontology (GO) and Kyoto Encyclopedia of Genes and Genomes (KEGG) pathway protein functions.

Finally, according to the results of functional annotation, the proteins with dysregulated Kla levels related to glucose metabolism, lipid metabolism and the cell cycle were analyzed by a heatmap.

Immunoblot analysis and immunoprecipitation (IP)

For immunoblot analysis, left ventricles from hearts at different time points were homogenized in RIPA buffer containing protease inhibitor PMSF (1 mM) and cocktails (04693132001, Roche, Switzerland) and were boiled for 5 mins. Proteins were separated by SDS−PAGE and transferred to a PVDF membrane (Roche). Membranes were blocked with 5% nonfat milk in PBST (PBS + 0.1% Tween 20) and then incubated with the indicated primary antibody overnight at 4°C. Bound primary antibodies were detected by HRP-conjugated secondary antibodies and chemiluminescent substrate. For IP, the hearts were homogenized in IP buffer containing cocktail and PMSF, and the lysates were centrifuged at 12000 rpm for 15 min at 4°C. Then, the supernatant was blocked with IgG (corresponding to the primary antibody) and protein A/G agarose beads (Santa Cruz, sc-2003; USA) for 4 h at 4°C and then centrifuged at 1000 × g for 5 min at 4°C. The supernatant was incubated with the primary antibody overnight at 4°C, and the immune complex was immunoprecipitated by protein A/G beads for 4 h at 4°C. The protein-antibody-bead complex was collected and washed with IP buffer, and finally, the protein was detected by immunoblotting. PKM (15822-1-AP, Proteintech), ACADL (17526-1-AP, Proteintech), ACAT1 (16215-1-AP, Proteintech), ACADVL (sc-376239, Santa Cruz), PFKM (55028-l-AP, Proteintech), NPM1 (60096-1-Ig, Proteintech), and 14-3-3z (sc-293415, Santa Cruz) were used in the IP and immunoblot analysis.

Database search

The mass spectrometry proteomics data have been deposited to the ProteomeXchange Consortium via the PRIDE[38] partner repository with the dataset identifier PXD039257. Submission details: Project

Name: Characterization of protein lactylation in relation to cardiac metabolic reprogramming in neonatal mouse hearts. Project accession: PXD039257; Project DOI: Not applicable. Reviewer account details: Username: reviewer_pxd039257@ebi.ac.uk; Password: bmkxICq1. The resulting MS/MS data were processed using Maxquant search engine (v.1.6.15.0). Tandem mass spectra were searched against the human SwissProt database (20422 entries) concatenated with reverse decoy database. Trypsin/P was specified as cleavage enzyme allowing up to 2 missing cleavages. The mass tolerance for precursor ions was set as 20 ppm in first search and 5 ppm in main search, and the mass tolerance for fragment ions was set as 0.02 Da. Carbamidomethyl on Cys was specified as fixed modification, and acetylation on protein N-terminal and oxidation on Met were specified as variable modifications. FDR was adjusted to < 1%.

Declarations

Supplementary information

Supplementary material is available at *BMC Genomics* online.

Ethics approval and consent to participate

All experimental protocols were approved by the Institutional Animal Ethics Committee of Model Animal Research Center of Nanjing University, Nanjing, China.

All methods were carried out in accordance with relevant guidelines and regulations.

All methods are reported in accordance with ARRIVE guidelines.

Consent for publication

Not applicable.

Availability of data and materials

The mass spectrometry proteomics data have been deposited to the ProteomeXchange Consortium via the PRIDE partner repository with the dataset identifier PXD039257. Submission details: Project Name: Characterization of protein lactylation in relation to cardiac metabolic reprogramming in neonatal mouse hearts. Project accession: PXD039257; Project DOI: Not applicable. Reviewer account details: Username: reviewer_pxd039257@ebi.ac.uk; Password: bmkxICq1. The authors declare that all relevant data of this study are available within the article or from the corresponding author upon reasonable request.

Competing interests

The authors declare no competing interests.

Author contributions

Chaojun Li and Tongyu Zhang designed the experiments and wrote the paper. Tongyu Zhang and Yingxi Zhu performed experiments. Xiaochen Wang, Danyang Chong, Haiquan Wang, Dandan Bu and Mengfei Zhao provided materials and methodology support. All authors have read and agreed to the published version of the manuscript.

References

1. Heidenreich PA, Trogdon JG, Khavjou OA, Butler J, Dracup K, Ezekowitz MD, Finkelstein EA, Hong Y, Johnston SC, Khera A, et al. Forecasting the future of cardiovascular disease in the United States: a policy statement from the American Heart Association. Circulation. 2011;123(8):933–44.

2. Roth GA, Mensah GA, Johnson CO, Addolorato G, Ammirati E, Baddour LM, Barengo NC, Beaton AZ, Benjamin EJ, Benziger CP, et al. Global Burden of Cardiovascular Diseases and Risk Factors, 1990–2019: Update From the GBD 2019 Study. J Am Coll Cardiol. 2020;76(25):2982–3021.

3. Peoples JN, Saraf A, Ghazal N, Pham TT, Kwong JQ. Mitochondrial dysfunction and oxidative stress in heart disease. Exp Mol Med. 2019;51(12):1–13.

4. Takahashi E, Doi K. Impact of diffusional oxygen transport on oxidative metabolism in the heart. Jpn J Physiol. 1998;48(4):243–52.

5. Keating ST, El-Osta A. Epigenetics and metabolism. Circ Res. 2015;116(4):715–36.

6. Pohjoismaki JL, Goffart S. The role of mitochondria in cardiac development and protection. Free Radic Biol Med. 2017;106:345–54.

7. Kordalewska M, Markuszewski MJ. Metabolomics in cardiovascular diseases. J Pharm Biomed Anal. 2015;113:121–36.

8. Zhou B, Tian R. Mitochondrial dysfunction in pathophysiology of heart failure. J Clin Invest. 2018;128(9):3716–26.

9. Piquereau J, Ventura-Clapier R. Maturation of Cardiac Energy Metabolism During Perinatal Development. Front Physiol. 2018;9:959.

10. Bartelds B, Gratama JW, Knoester H, Takens J, Smid GB, Aarnoudse JG, Heymans HS, Kuipers JR. Perinatal changes in myocardial supply and flux of fatty acids, carbohydrates, and ketone bodies in lambs. Am J Physiol. 1998;274(6):H1962–1969.

11. Kolwicz SC Jr, Purohit S, Tian R. Cardiac metabolism and its interactions with contraction, growth, and survival of cardiomyocytes. Circ Res. 2013;113(5):603–16.

12. Bartelds B, Knoester H, Beaufort-Krol GC, Smid GB, Takens J, Zijlstra WG, Heymans HS, Kuipers JR. Myocardial lactate metabolism in fetal and newborn lambs. Circulation. 1999;99(14):1892–7.

13. Bartelds B, Knoester H, Smid GB, Takens J, Visser GH, Penninga L, van der Leij FR, Beaufort-Krol GC, Zijlstra WG, Heymans HS, et al. Perinatal changes in myocardial metabolism in lambs. Circulation. 2000;102(8):926–31.

14. Singer D, Muhlfeld C. Perinatal adaptation in mammals: the impact of metabolic rate. Comp Biochem Physiol A Mol Integr Physiol. 2007;148(4):780–4.

15. Lehman JJ, Kelly DP. Transcriptional activation of energy metabolic switches in the developing and hypertrophied heart. Clin Exp Pharmacol Physiol. 2002;29(4):339–45.

16. Porrello ER, Mahmoud AI, Simpson E, Hill JA, Richardson JA, Olson EN, Sadek HA. Transient regenerative potential of the neonatal mouse heart. Science. 2011;331(6020):1078–80.

17. Porrello ER, Mahmoud AI, Simpson E, Johnson BA, Grinsfelder D, Canseco D, Mammen PP, Rothermel BA, Olson EN, Sadek HA. Regulation of neonatal and adult mammalian heart regeneration by the miR-15 family. Proc Natl Acad Sci U S A. 2013;110(1):187–92.

18. Tzahor E, Poss KD. Cardiac regeneration strategies: Staying young at heart. Science. 2017;356(6342):1035–9.

19. Uygur A, Lee RT. Mechanisms of Cardiac Regeneration. Dev Cell. 2016;36(4):362–74.

20. Chong D, Gu Y, Zhang T, Xu Y, Bu D, Chen Z, Xu N, Li L, Zhu X, Wang H, et al. Neonatal ketone body elevation regulates postnatal heart development by promoting cardiomyocyte mitochondrial maturation and metabolic reprogramming. Cell Discov. 2022;8(1):106.

21. Zhang D, Tang Z, Huang H, Zhou G, Cui C, Weng Y, Liu W, Kim S, Lee S, Perez-Neut M, et al. Metabolic regulation of gene expression by histone lactylation. Nature. 2019;574(7779):575–80.

22. Du J, Zheng L, Gao P, Yang H, Yang WJ, Guo F, Liang R, Feng M, Wang Z, Zhang Z, et al. A small-molecule cocktail promotes mammalian cardiomyocyte proliferation and heart regeneration. Cell Stem Cell. 2022;29(4):545–558e513.

23. Popov IK, Hiatt SM, Whalen S, Keren B, Ruivenkamp C, van Haeringen A, Chen MJ, Cooper GM, Korf BR, Chang C. A YWHAZ Variant Associated With Cardiofaciocutaneous Syndrome Activates the RAF-ERK Pathway. Front Physiol. 2019;10:388.

24. Angrand PO, Segura I, Volkel P, Ghidelli S, Terry R, Brajenovic M, Vintersten K, Klein R, Superti-Furga G, Drewes G, et al. Transgenic mouse proteomics identifies new 14-3-3-associated proteins involved in cytoskeletal rearrangements and cell signaling. Mol Cell Proteomics. 2006;5(12):2211–27.

25. Ganguly S, Weller JL, Ho A, Chemineau P, Malpaux B, Klein DC. Melatonin synthesis: 14-3-3-dependent activation and inhibition of arylalkylamine N-acetyltransferase mediated by phosphoserine-205. Proc Natl Acad Sci U S A. 2005;102(4):1222–7.

26. Hermeking H, Benzinger A. 14-3-3 proteins in cell cycle regulation. Semin Cancer Biol. 2006;16(3):183–92.

27. Doppler SA, Deutsch MA, Serpooshan V, Li G, Dzilic E, Lange R, Krane M, Wu SM. Mammalian Heart Regeneration: The Race to the Finish Line. Circ Res. 2017;120(4):630–2.

28. Badolia R, Ramadurai DKA, Abel ED, Ferrin P, Taleb I, Shankar TS, Krokidi AT, Navankasattusas S, McKellar SH, Yin M, et al. The Role of Nonglycolytic Glucose Metabolism in Myocardial Recovery Upon Mechanical Unloading and Circulatory Support in Chronic Heart Failure. Circulation. 2020;142(3):259–74.

29. Liu S, Tang L, Zhao X, Nguyen B, Heallen TR, Li M, Wang J, Wang J, Martin JF. Yap Promotes Noncanonical Wnt Signals From Cardiomyocytes for Heart Regeneration. Circ Res. 2021;129(8):782–97.

30. Padin-Iruegas ME, Misao Y, Davis ME, Segers VF, Esposito G, Tokunou T, Urbanek K, Hosoda T, Rota M, Anversa P, et al. Cardiac progenitor cells and biotinylated insulin-like growth factor-1 nanofibers improve endogenous and exogenous myocardial regeneration after infarction. Circulation. 2009;120(10):876–87.

31. Nakada Y, Canseco DC, Thet S, Abdisalaam S, Asaithamby A, Santos CX, Shah AM, Zhang H, Faber JE, Kinter MT, et al. Hypoxia induces heart regeneration in adult mice. Nature. 2017;541(7636):222–7.

32. Magadum A, Singh N, Kurian AA, Munir I, Mehmood T, Brown K, Sharkar MTK, Chepurko E, Sassi Y, Oh JG, et al. Pkm2 Regulates Cardiomyocyte Cell Cycle and Promotes Cardiac Regeneration. Circulation. 2020;141(15):1249–65.

33. Li L, Chen K, Wang T, Wu Y, Xing G, Chen M, Hao Z, Zhang C, Zhang J, Ma B, et al. Glis1 facilitates induction of pluripotency via an epigenome-metabolome-epigenome signalling cascade. Nat Metab. 2020;2(9):882–92.

34. Irizarry-Caro RA, McDaniel MM, Overcast GR, Jain VG, Troutman TD, Pasare C. TLR signaling adapter BCAP regulates inflammatory to reparatory macrophage transition by promoting histone lactylation. Proc Natl Acad Sci U S A. 2020;117(48):30628–38.

35. Hagihara H, Shoji H, Otabi H, Toyoda A, Katoh K, Namihira M, Miyakawa T. Protein lactylation induced by neural excitation. Cell Rep. 2021;37(2):109820.

36. Zhang N, Jiang N, Yu L, Guan T, Sang X, Feng Y, Chen R, Chen Q. Protein Lactylation Critically Regulates Energy Metabolism in the Protozoan Parasite Trypanosoma brucei. Front Cell Dev Biol. 2021;9:719720.

37. Wan N, Wang N, Yu S, Zhang H, Tang S, Wang D, Lu W, Li H, Delafield DG, Kong Y, et al. Cyclic immonium ion of lactyllysine reveals widespread lactylation in the human proteome. Nat Methods. 2022;19(7):854–64.

38. Perez-Riverol Y, Bai J, Bandla C, Garcia-Seisdedos D, Hewapathirana S, Kamatchinathan S, Kundu DJ, Prakash A, Frericks-Zipper A, Eisenacher M, et al. The PRIDE database resources in 2022: a hub for mass spectrometry-based proteomics evidences. Nucleic Acids Res. 2022;50(D1):D543–52.
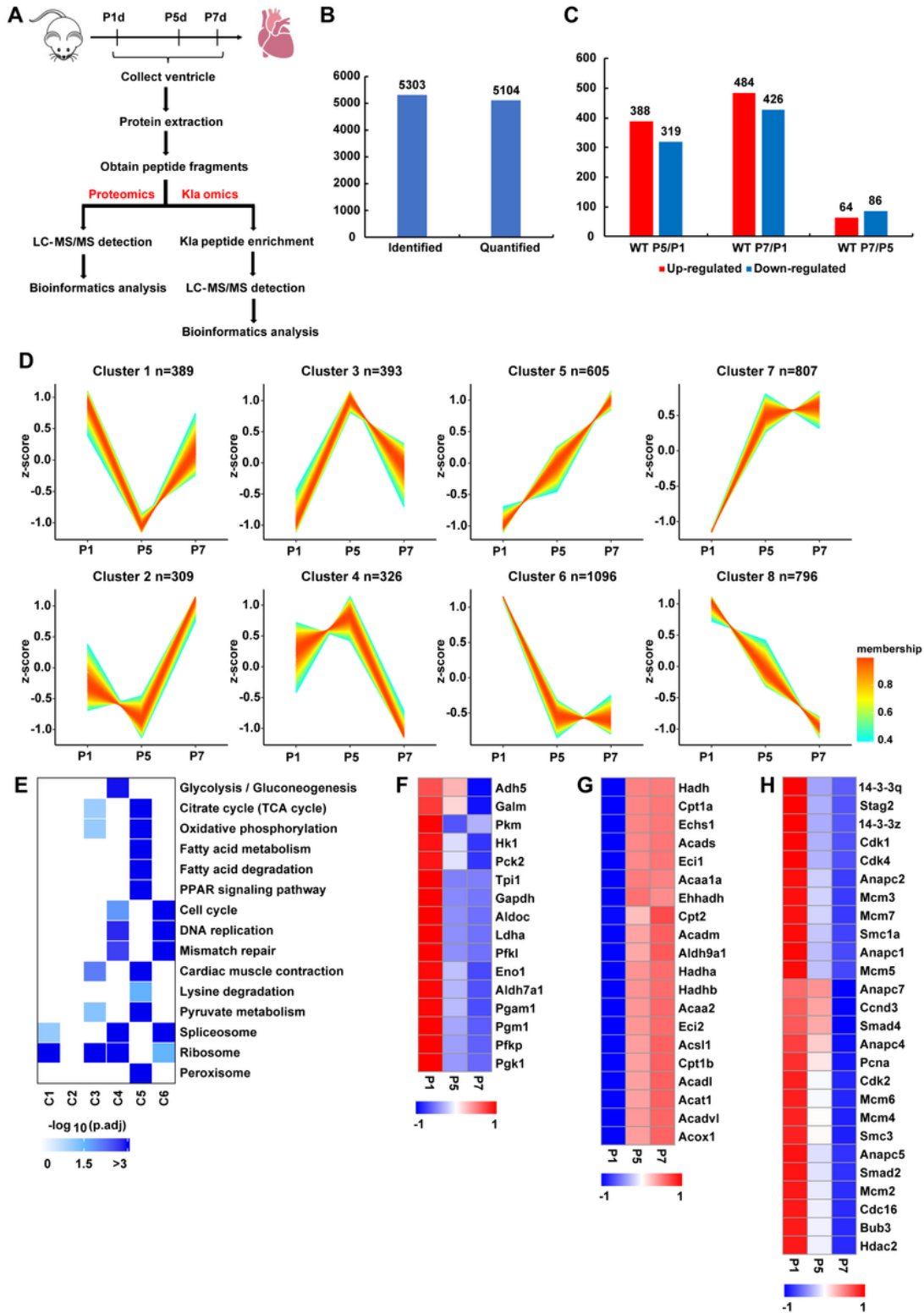
Figures

Figure 1

Bioinformatics analyses of general proteomics showed metabolic reprogramming in neonatal hearts. **A:** The schematic workflow of proteomics and Kla omics; **B:** Summary of identified and quantified proteins; **C:** Summary of dysregulated proteins in neonatal heart; **D:** Series test of cluster (STC) analysis of the

4721 differentially expressed proteins; **E:** KEGG pathway analysis of the 6 clusters; **F-H:** Proteins abundance of glycolytic enzyme **(F)**, FAO related proteins **(G)** and cell cycle related proteins **(H)**.
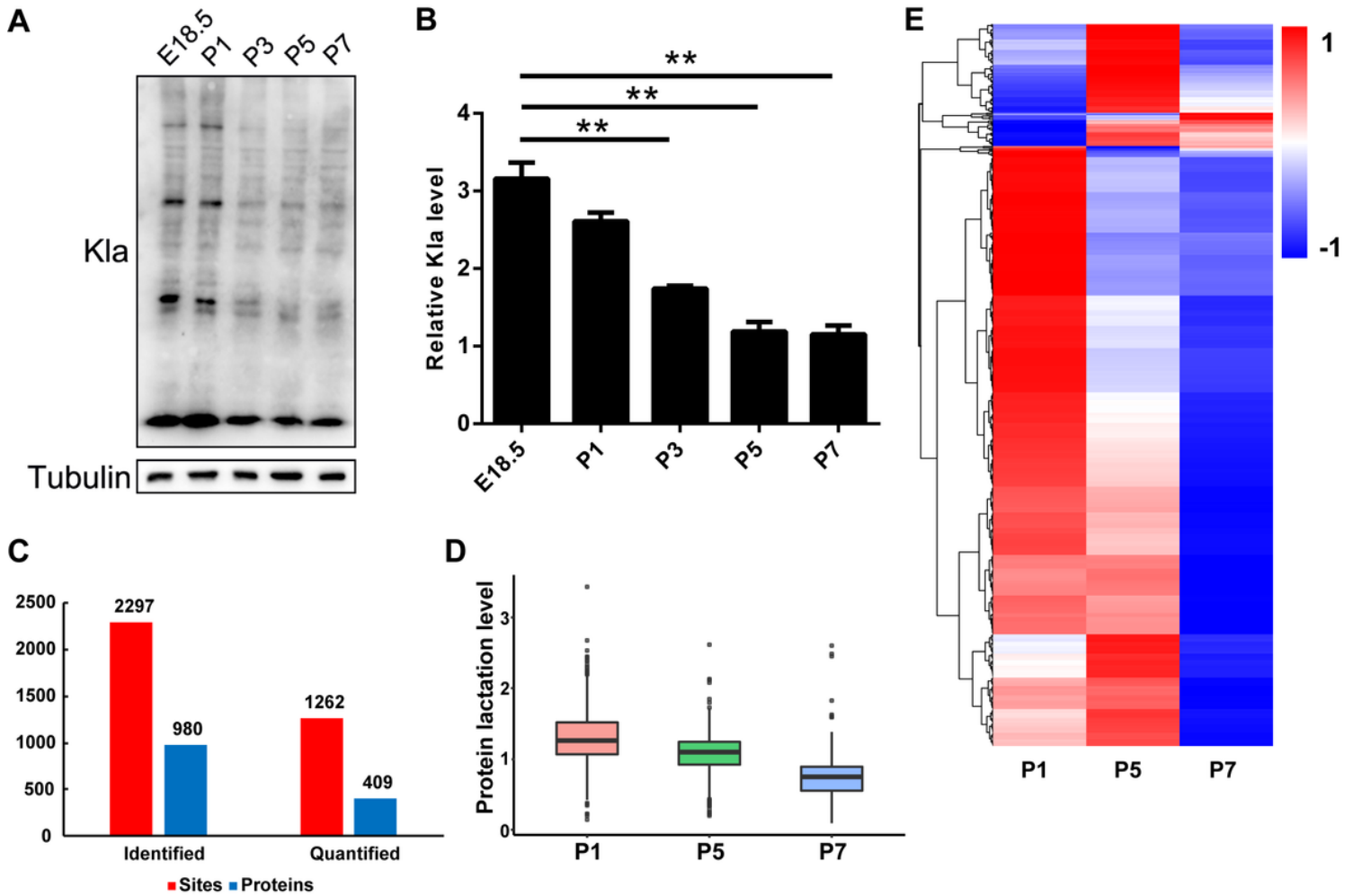
Figure 2

The globalprotein Kla level was decreased with metabolic reprogramming during the perinatal stage. **A**: Western blot analysis of global Kla abundance in perinatal hearts; **B**: Quantified analysis of Figure 2A; **C:**Summary of identified and quantified lactylated proteins and Kla sites; **D:**Protein lactylation level after standardization. **E:** Heatmap of Kla levels in P1, P5 and P7 hearts.
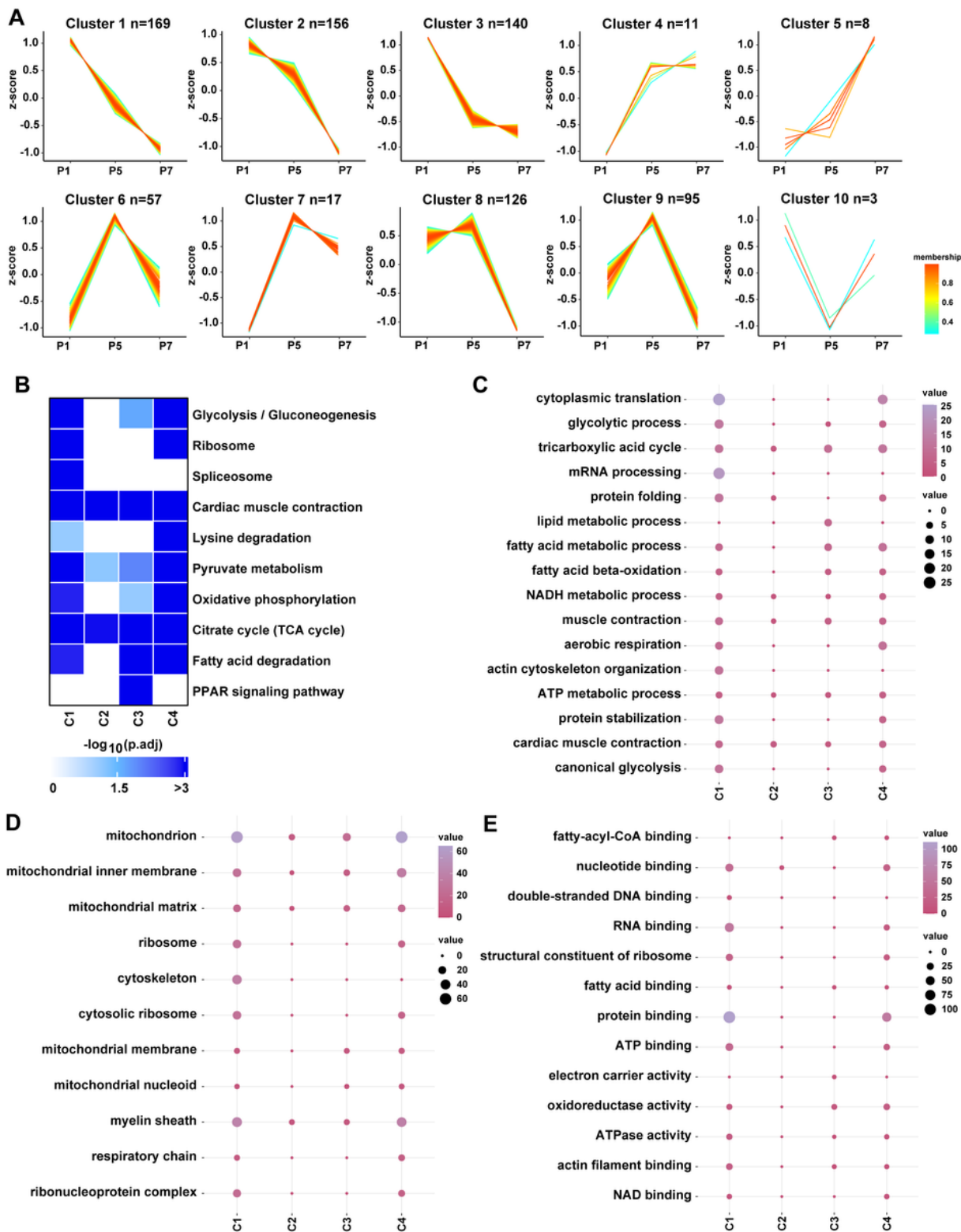
Figure 3

Functional enrichment analysis of proteins with dysregulated Kla sites. **A:** STC analysis of the 782 differentially modified Kla sites; **B:** KEGG pathway analysis of the 4 clusters of Kla omics; **C-E:** Graphical representation of GO biological process category **(C)**, cellular component category **(D)** and molecular function category **(E)** of C1-C4.
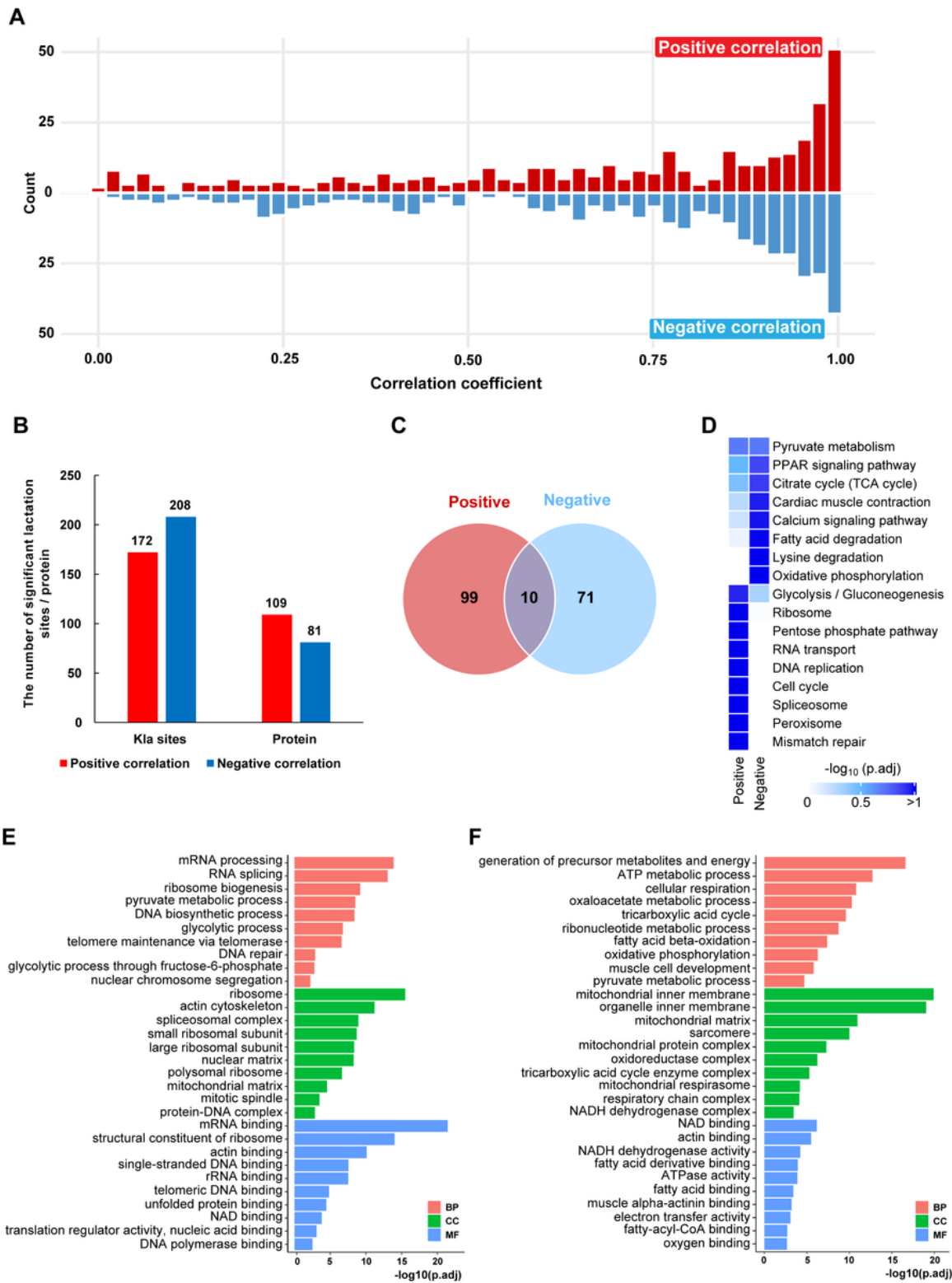
Figure 4

Glycolysis and cell proliferation showed positive correlation between proteomics and Kla omics while FAO showed negative correlation. **A:** Correlation coefficient analysis between protein level and Kla level of the dysregulated Kla sites; **B:** The number of significant correlated Kla sites/proteins when setting correlation coefficient 0.8; **C:** Venn diagram of positive correlation group and negative correlation group;

D: KEGG pathway analysis of positive and negative correlation groups; **E-F:** Functional enrichment of positive correlation group (**E**) and negative correlation group (**F**).
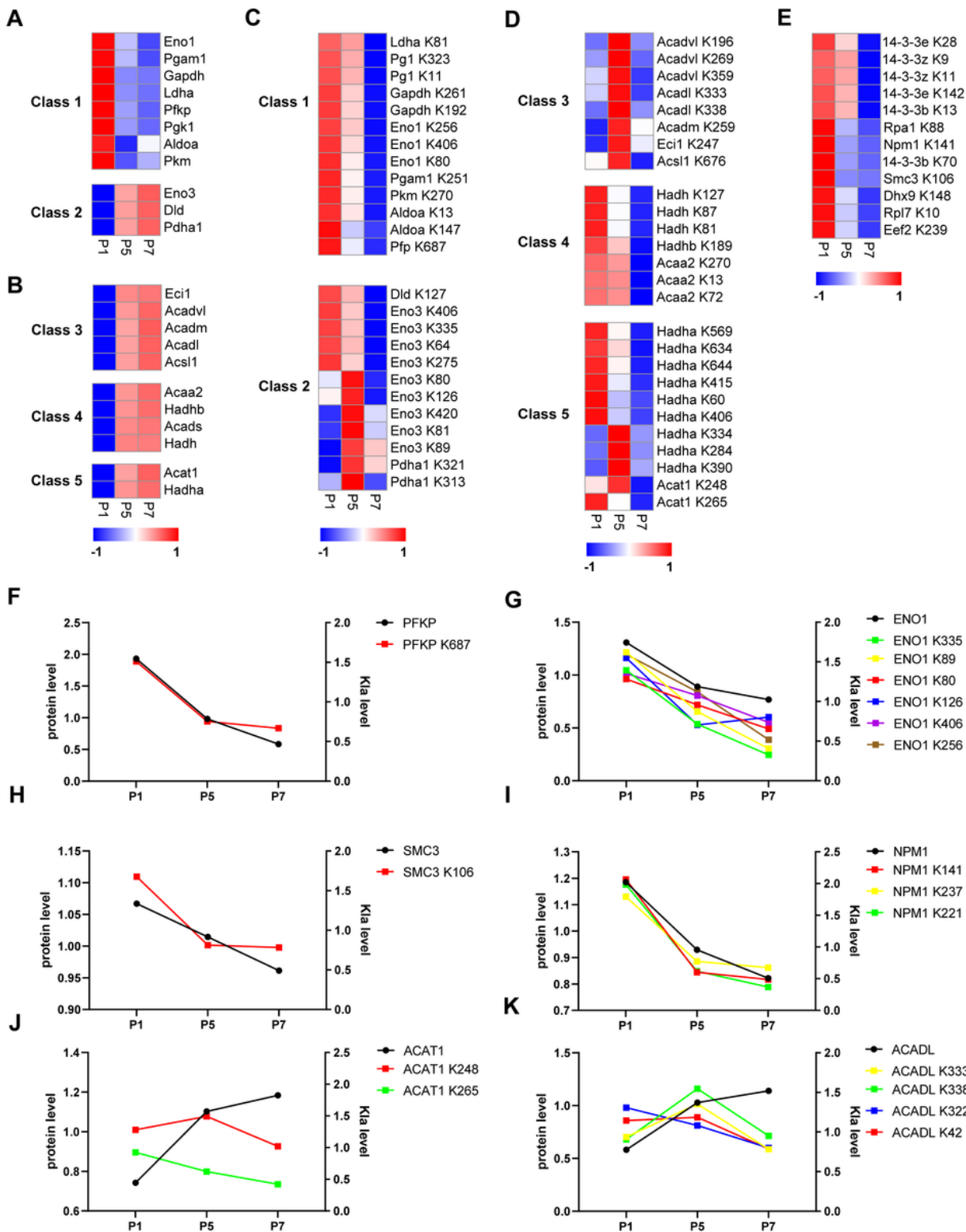

Figure 5

Altered Kla proteins enriched in metabolic pathways. **A:**Protein abundance of glycolytic proteins; **B:** Protein abundance of FAO proteins; **C:** Kla level of glycolytic proteins; **D:** Kla level of FAO proteins; **E:** Kla

level of cell cycle-related proteins. **F-K:** The protein levels and Kla levels of selected proteins at P1, P5 and P7.
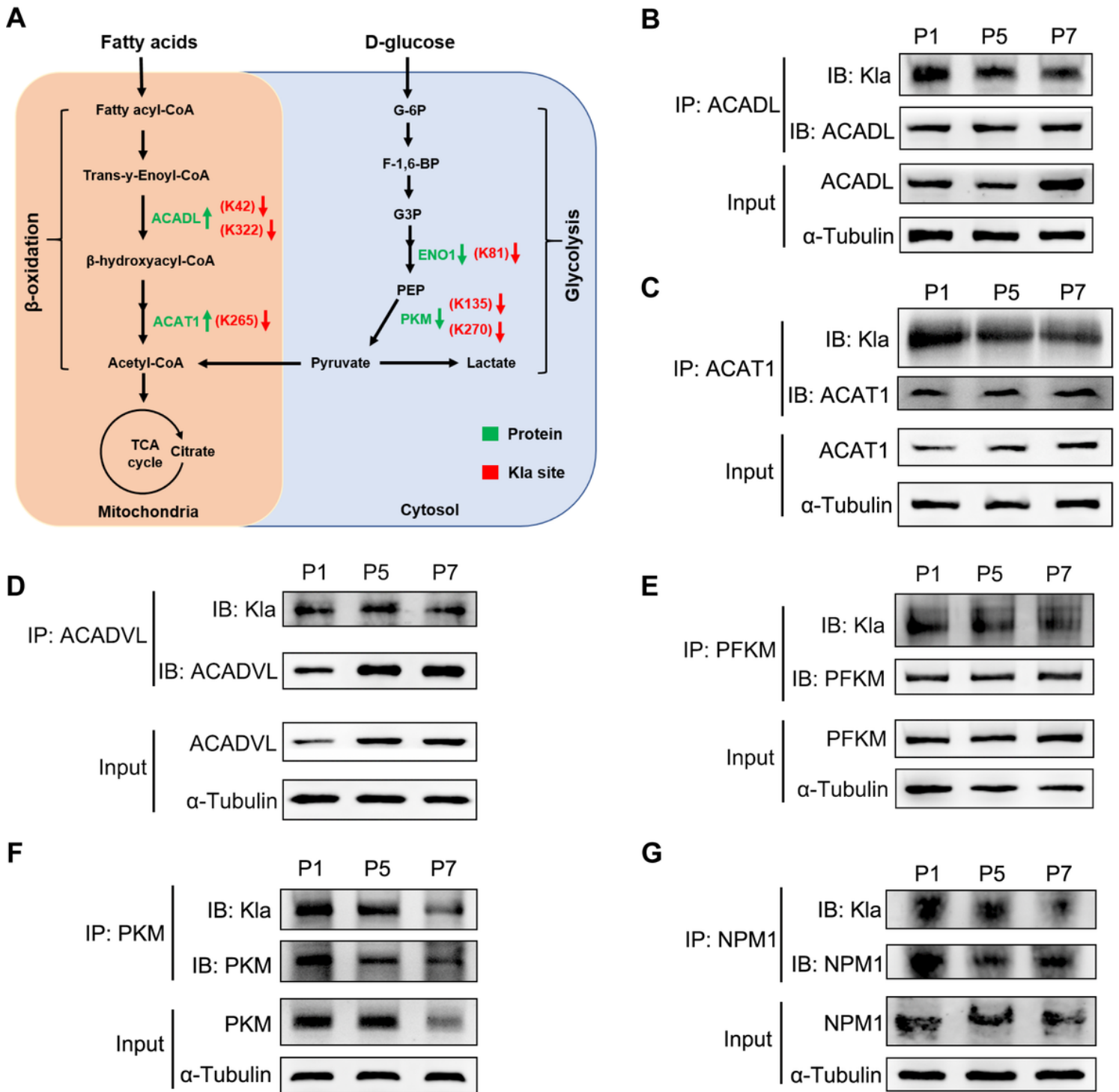

Figure 6

Verification of proteins with differentially regulated Kla sites. **A:** Diagram of the glycolysis and fatty acid β-oxidation pathway with key enzymes characterized by functional enrichment analysis; **B-G:** The Kla abundance and protein level of selected proteins detected by coimmunoprecipitation and Western blot.

Supplementary Files

This is a list of supplementary files associated with this preprint. Click to download.

- SupplementaryInfoFile1.xlsx
- SupplementaryInfoFile2.xlsx
- Supplementaryinformation.pdf